



ISSN: 0067-2904

Biosynthesis, characterization, and antibiofilm activity of copper-oxide nanoparticles using a mixture of *Klebsiella pneumonia* and *Staphylococcus aureus* supernatant

Atika Ali Arrak Al-tamimi*, Hassan Majeed Rasheed

Department of Biology, College of Science, University of Baghdad, Baghdad, Iraq.

Received: 28/2/2025

Accepted: 28/5/2025

Published: xx

Abstract

Biosynthesis of copper oxide nanoparticles using the extracellular mixture solution of Gram-negative bacteria *Klebsiella pneumonia* and Gram-positive bacteria *Staphylococcus aureus* acted as a reducing and capping agent to stabilize and prevent the aggregation of the biosynthesized nanoparticles. CuO NPs are characterized by UV-visible, FTIR, AFM, FE-SEM, and XRD, and tested for their antibiofilm activity against *Pseudomonas aeruginosa*. The biofilm capability was demonstrated with the microtiter plate method. The antibiotic susceptibility of *P. aeruginosa* exhibits resistance to Piperacillin, Nitrofurantoin, and Levofloxacin. While sensitive to Cefepime, Piperacillin-Tazobactam, and Imipenem. The antibiofilm activity of CuONPs illustrates that all the prepared concentrations exhibit antibiofilm efficacy against *P. aeruginosa* biofilm, and 50 mg/ml was correlated with the highest activity. The concentrations 25, 12.5, and 6.25 mg/ml reduced the biofilm intensity to a weak level, and the last effect was associated with a 6.25 mg/ml concentration.

Keywords: Bio-synthesized, Copper-Oxide, Nanoparticles, *Klebsiella pneumonia*, *Staphylococcus aureus*, *Pseudomonas aeruginosa*.

التخليق الحيوي , التوصيف, و الفعالية المضادة للأغشية الحيوية لدقائق اوكسيد النحاس النانوية باستخدام الراشح لخليط من الكلبسيلا الرئوية و المكورات الذهبية العنقودية

عاتكه علي عراك التميمي* ، حسن مجيد رشيد

قسم علوم الحياة، كلية العلوم، جامعة بغداد ، بغداد ، العراق

الخلاصة

التخليق الحيوي لدقائق أكسيد النحاس النانوية باستخدام الراشح البكتيري لمزيج من البكتيريا سالبة لصبغها كرام الكلبسيلا الرئوية و موجبة لصبغة المكورات العنقودية الذهبية حيث يعمل الراشح البكتيري كعامل مختزل و مغط للجسيمات لغرض جعلها أكثر استقراراً و منع تجمع الجسيمات النانوية المخلفة حيوياً . تم توصيف دقائق أكسيد النحاس النانوية باستخدام عدة تقنيات، وهي : مطياف الأشعة المرئية، مطياف الأشعة تحت الحمراء، الفحص المجهرى للقوة الذرية، جهاز حيود الأشعة السينية، و المجهر الإلكتروني الماسح. تم اختبار فعالية هذه الجسيمات ضد الأغشية الحيوية لبكتريا الزائفة

*Email: atika.ali1802a@sc.uobaghdad.edu.iq

الزنجارية. وقد تم اثبات قدرة هذه البكتريا على تكوين الأغشية الحيوية باستخدام طريقة صفيحة المعايرة الدقيقة. اظهرت الزانفة الزنجارية مقاومة للمضادات الحيوية بيبراسيلين, نيتروفورانتونين, و ليفوفلوكساسين, بينما كانت حساسة لمضادات سيفيبيم, بيبراسيلين-تازوباكتام, و ايميبينييم. أما الفعالية المضادة للأغشية الحيوية لا كسيد النحاس النانوية, فقد اظهرت جميع التراكيز المحضرة تأثيرا مضادا للأغشية الحيوية لبكتريا الزانفة الزنجارية, حيث كانت اعلى فعالية عند تركيز 50 ميكروغرام / مل , في حين كان كل من تركيز 25 و 12.5 و 6.25 ميكروكرام / مل ادت الى خفض شدة الاغشية الحيوية لمستوى ضعيف. واقل فعالية كانت عند تركيز 6.25 ميكروغرام/مل.

Introduction

Green synthesis methods can create nanoparticles ranging in diameter from 1 nm to 100 nm. Nanoparticles have unique physical and chemical properties that make them ideal for a variety of applications in industries, including electronics, environmental remediation, and healthcare[1]. There are numerous chemical and physical techniques for creating metal oxide nanoparticles, such as laser ablation, sol-gel, ion sputtering, and chemical reduction. However, all of these synthesized processes have a number of drawbacks, including the need for expensive, dangerous chemicals, high energy consumption, and the creation of hazardous byproducts that eventually pollute the environment [2]. Consequently, the green synthesis method (biosynthesis) has garnered significant attention from researchers due to its utilization of eco-friendly components such as plants and microbes[3]. Microorganisms are utilized for nanomaterial manufacturing due to their unique biological processes that yield powerful proteins, which operate as biological manufacturing facilities to regulate the properties of nanomaterials and maintain their stability under extreme circumstances. Microbes employ reducing agents, also known as enzymes, that can transform precursors into metallic nanoparticles. Microbes are important manufacturers of nanoparticles that have the capacity to detoxify heavy metals[4]. *Klebsiella pneumoniae* is a Gram-negative bacterium belonging to the Enterobacteriaceae family and characterized as an opportunistic pathogen[5]. *K. pneumoniae* is found in the mucosal epithelium of several mammal species, the gastrointestinal tract, the respiratory tract, the urinary system, and the udder[6]. These healthcare disorders can cause a variety of diseases, especially in people with compromised immune systems. *K. pneumoniae* illnesses are particularly common in medical facilities[7]. *K. pneumoniae* exhibits the ability to biosynthesize nanoparticles that are characterized by several features, such as being contaminant-free and eco-friendly. *K. pneumoniae* acts as a reducing and stability-stabilizing agent for nanoparticle production. It also exhibits antibacterial action against Gram-negative and Gram-positive bacteria[8]. *Staphylococcus aureus* is one of the most important Gram-positive bacteria recognized by its ability to withstand diverse circumstances [9]. *S. aureus* is considered one of the most life-threatening microorganisms that are responsible for a wide range of diseases, including mild infections, for instance, boils and pimples, and serious infections, such as sepsis and bacteremia [10]. Additionally, one of the most important strategies of *S. aureus* to avoid immunological recognition is the secretion of several enzymes and toxins in order to develop the infection and ensure the proliferation of cells and the infected tissues[11]. The metabolic compounds that were secreted from *S. aureus* (bacterial supernatant) were utilized to synthesize metal nanoparticles, such as silver nanoparticles (Ag NPs)[12]. *Pseudomonas aeruginosa* is one of the most common Gram-negative bacteria that is associated with most hospital-acquired infections and death in people with immunological disorders, including cancer patients, surgical patients, people who have had serious burns, and those infected with Human immunodeficiency virus (HIV)[13]. *P. aeruginosa* is the most investigated organism isolated from different clinical sources, including urine, burns, and wounds[14]. One significant type of microbial life is biofilms. The biofilm proved to be the resident microorganisms shield against reactive oxygen species, host immune response, and metallic cations and provided pathogenicity factors that contribute to illness and death[15].

Materials and Methods

Sample collection

One hundred and seventy-seven clinical samples were collected from patients with nasal and urinary tract infections (UTIs), burn and wound patients residing in the Al-Kadhimiya Teaching Hospital of Baghdad city during the period from September 2024 to January 2025.

*Isolation and identification of *K. pneumoniae**

For the isolation of *K. pneumoniae* from wound, burn, and UTIs, 89 collected swabs were cultured on MacConkey agar and incubated for 24 hr. at 37°C. *K. pneumoniae* identification based on the morphological characteristics of the combination of culture media (chromogenic agar, Eosin methylene blue (EMB), and MacConkey agar), biochemical tests, and the Vitek 2 compact system (Biomerien/France)[16].

*Isolation and identification of *S. aureus**

The clinical samples of *S. aureus* were isolated from nasal and UTI infection patients on Mannitol Salt Agar (MSA) and incubated at 37°C for 24 hr. Identification of *S. aureus* through inoculation on several culture media, including blood agar, chromogenic UTI, milk agar, biochemical tests, and the Vitek 2 system[17].

Production of extracellular extracts

A colony of *S. aureus* and a colony of *K. pneumoniae* were co-inoculated in the same nutrient broth, incubated at 37°C for 24 hours, and subsequently centrifuged for 20 minutes at 8000 rpm. Only the bacterial supernatant was recovered, while the pellet was discarded[18].

Biosynthesis of copper-oxide nanoparticles using extracellular extract.

Copper oxide nanoparticles were biosynthesized by modified procedures according to Yaaqoob [19]. Copper chloride (CuCl₂) has been used to create copper oxide nanoparticles from extracellular compounds in the supernatant of the mixture of *K. pneumoniae* and *S. aureus*. When mixing two types of bacteria, each bacterium produces compounds that other bacteria may not produce, and when they interact together, it leads to the production of unique compounds that facilitate the formation of nanomaterials or make them have different properties, such as size, shape, stability, and antibacterial effectiveness. The procedure involves 10 grams of CuCl₂ being dissolved in 100 ml of the bacterial extracellular products and kept in a shaker at room temperature overnight in dark conditions. After shaking, the mixture was centrifuged at 8000 rpm for 20 min and washed with deionized distilled water two times, finally dried at 37°C in the incubator for three days to gain green powder, and stored in dark conditions for later use.

Characterization of nanoparticles

The copper oxide nanoparticles were characterized using multiple techniques, including ultraviolet-visible (UV-Visible) using a UV-visible spectrophotometer (Shimadzu, Japan), Field Transform- Infrared Spectroscopy (FT-IR) using a Shimadzu 8400 FT-IR spectrometer, and Atomic Force Microscopy (AFM). These tests were performed in Iraq, Baghdad, at Baghdad University, College of Science, Department of Chemistry. In addition, Field Emission-Scanning Electron Microscopy (FE-SEM) was performed using a scanning electron microscope, and X-ray diffraction (XRD) using an X-ray diffractometer. These tests were performed in the Ministry of Science and Technology, Baghdad, Iraq.

Isolation and identification of bacterial isolates

For *P. aeruginosa* isolation from UTI patients, the swabs were inoculated in brain heart infusion broth and incubated at 37°C overnight. Then, it is isolated through culture on a

ceramide agar for 24 hr at 37°C and identified via the morphological characters that have been demonstrated on a combination of culture media and the Vitek 2 automatic identification system [20].

Antibiotic sensitivity test of Pseudomonas aeruginosa

The Kirby-Bauer disc diffusion method was used to conduct the antibiotic susceptibility test. The antibiotic discs were implemented with Levofloxacin (5 µg), Piperacillin (100 µg), Piperacillin- Tazobactam (100/10 µg), Cefepime (30 µg), Imipenem (30 µg), Amikacin (30 µg), and Norfloxacin (10 µg). The density of the suspensions was adjusted to the 0.5 McFarland turbidity standard, which is equivalent to roughly 1.5×10^8 CFU/mL. Sterile cotton swabs were used to spread suspensions to the Muller-Hinton agar plate's surface. Prior to adding the antibiotic discs, the plates were dried, and they were then incubated at 37° C for 16–18 hours. Measurements were made of the inhibition zone diameters surrounding the discs. The Clinical Laboratory Standards Institute's criteria for interpreting data were followed (CLSI, 2024)[21].

Detection of biofilm formation (Quantitatively)

P. aeruginosa was cultured on brain heart infusion broth (BHI broth) overnight. Two hundred microliters of BHI with 1% glucose were used to dilute the suspensions 1:100. Following that, they were put into the sterile U-shaped bottom 96-well polystyrene microplates. After a 24-hour incubation period at 37°C, the wells were gently cleaned three times with distilled water. After fixing adherent biofilms for 15 minutes with 99% methanol, the liquids were taken out, and the plate was allowed to air dry. After staining the biofilms for 15 minutes at room temperature with 200 µL of 0.1% crystal violet, they were rinsed with water and left to dry. To de-stain the biofilm, in each well, 200 µL of 95% ethanol was applied for 10 minutes. The optical density (OD) was determined with a microtiter plate reader at 630 nm. Every experiment was carried out three times in triplicate[22]. Based on the mean OD as they relate to the OD_c values, the isolates were divided into four groups, as shown in Table 1[23].

Table 1: Classification of the bacterial biofilm production with the 96-well microtiter plate method

Mean of OD	The biofilm degree
$OD \leq OD_c$	non-biofilm producer
$OD > OD_c$, but $\leq 2 \times OD_c$	weak biofilm producer
$OD > 2 \times OD_c$, but $\leq 4 \times OD_c$	moderate biofilm producer
$OD > 4 \times OD_c$	strong biofilm producer

OD_c = cutoff optical density, OD = optical density

Determine the minimum inhibitory concentration (MIC) of copper oxide nanoparticles

The minimum inhibitory concentration (MIC) of CuONPs against *P. aeruginosa* was determined using 96-well microtiter plate. The typical procedure involves 100 µl of double-stranded Muller Hinton broth (MHB) added to each well of the microtiter plate. The work solution of CuONPs was prepared by dissolving 1g of CuONPs in 10 ml of deionized distilled water. Serial two-fold dilutions were generated on a microtiter plate to make concentrations (50, 25, 12.5, 6.25, and 3.125 mg/ml). 100 µl of CuONPs solution was added to the well in column A and mix properly with a micropipette and take 100 µl of it to the next well, and the process repeats to the well in row H that has a 200 µl volume, and discard 100 µl of it to reach the final volume of 100 µl, and 10 µl bacterial broth (0.5 MacFarland turbidity standard) is added to each well except the negative control that contains the CuONPs solution only. The positive control contains 100 µl of MHB and 10 µl of bacteria that equal to 0.5 MacFarland.

And incubated at 37°C for 16-18 hr. 15 µl of resazurin dye was added to each well and incubated for 3 hr at 37°C and read with the naked eye [24].

Detection of antibiofilm activity of CuONPs

Pseudomonas aeruginosa isolate which multidrug resistance and strong biofilm producer, was used to detect of anti-biofilm efficacy of the biosynthesized CuONPs. The bacterial isolate cultured in Brain Heart Infusion broth (BHI) and incubated at 37°C for 24 hr. After the incubation, the turbidity of the bacterial suspension was equivalent to 0.5 McFarland turbidity standard. The CuONPs series concentrations (50, 25, 12.5, 6.25 and 3.125 mg/mL) were prepared. A 96-well microtiter plate was employed. 100 µL of standardized inoculum of *P. aeruginosa* was introduced into each well then, the plate was incubated at 37°C for 48 hr. Subsequent to the incubation period, 100 µL of each concentration of CuONPs was added to each well in triplicate to reach the final volume of 200 µL in each well. The plate was incubated for another 24 hr. at 37°C. Finally, the absorbance was measured for each well using a microplate reader at 650 nm [25, 26].

Results and Discussion

Isolation and identification

The current study demonstrates that sixty-five *K. pneumoniae* isolates produced large, mucoid, pink colonies on MacConkey agar. While on EMB agar, the isolates appeared as dark pink, smooth, mucoid colonies because of their ability to ferment lactose, and on chromogenic UTI agar, they produced blue to pink mucoid colonies due to their ability to produce beta-glycosidase that cleaves the chromogenic substance of the medium. Then the isolates were examined for the catalase biochemical test, which showed catalase-positive, as shown in Figure 1. These findings are in agreement with the results reported by Ali [27]. Additionally, all thirty *S. aureus* isolates exhibited the ability to ferment mannitol, resulting in a color change of phenol red to yellow. All isolates formed yellow colonies on MSA, as shown in Figure 2. While on blood agar, they produced beta-hemolysis (complete hemolysis surrounding the colonies) due to the ability to produce hemolysin enzyme; yellow colonies were observed on chromogenic UTI agar due to beta-glycosidase enzyme production; and on milk agar, a white halo formed due to protease enzyme production. All *S. aureus* isolates revealed positive results for both catalase and coagulase tests [28]. Finally, the VITEK II system confirms the identification of *K. pneumoniae* and *S. aureus*.

A total of 58 *P. aeruginosa* isolates were obtained from 108 urine samples (53.7%, 58/108), *P. aeruginosa* is considered an important responsible agent for UTIs, besides *Escherichia coli*, *K. pneumoniae*, *Enterococcus faecalis*, *Proteus mirabilis*, *Staphylococcus saprophyticus*, and others [29, 30].



Figure 1: The morphological characteristics of *Klebsiella pneumoniae* on some culture media (A-MacConkey agar, B-Eosin methylene blue agar, and C-Chromogenic UTI agar) and the D-catalase test, respectively.



Figure 2: *Staphylococcus aureus* on mannitol salt agar.

Antibiotic sensitivity test of Pseudomonas aeruginosa

For 58 isolates of *P. aeruginosa*, only 20 isolates were tested for antibiotic susceptibility. *P. aeruginosa*, which exhibited variations in their ability to resist different antibiotics. The present study exhibits the highest resistance against the Piperacillin antibiotic (30%), Norfloxacin, and Levofloxacin (10% of each). The intermediate bacterial resistance was demonstrated against Piperacillin and Levofloxacin (15% of each), and Norfloxacin (10%). All 20 of the bacterial isolates were susceptible to Amikacin, Cefepime, Piperacillin-Tazobactam, and Imipenem. The antibiotic sensitivity test of *P. aeruginosa* showed that only 2 of 20 bacterial isolates were MDR (multidrug-resistant). The results of the antibiotic susceptibility of the *P. aeruginosa* were demonstrated in Figures 3 and 4. *P. aeruginosa* exhibits resistance to multiple antibiotics due to the ability to produce resistance enzymes, such as beta-lactamase enzymes that break the beta-lactam ring of beta-lactam antibiotics, efflux pumps that extrude antibiotics from the cell, reduce the permeability of the outer membrane, and due to acquired resistance genes through horizontal gene transfer [31].

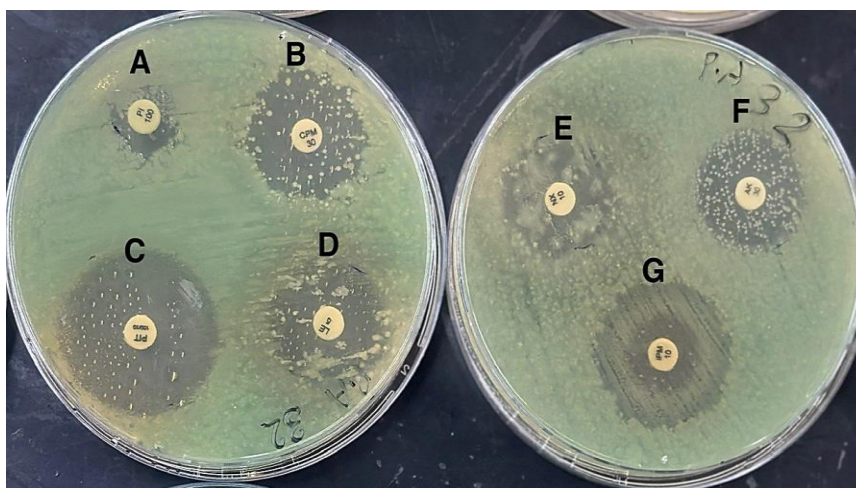


Figure 3: Results of antibiotic susceptibility test of *Pseudomonas aeruginosa* (A- Piperacillin, B- Cefepime, C- Piperacillin-tazobactam, D- Levofloxacin, E- Norfloxacin, F- Amikacin, and G- Imipenem).

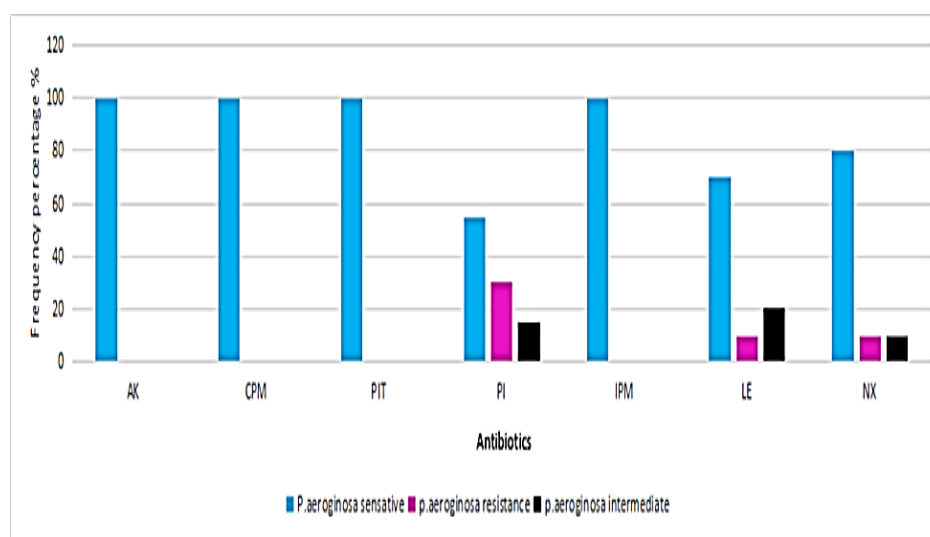


Figure 4: Results of the antibiotic susceptibility test of *P. aeruginosa*. The symptoms (AK, CPM, PIT, PI, IPM, LE, and NX) for Amikacin, Cefepime, Piperacillin-tazobactam, Piperacillin, Imipenem, Levofloxacin, and Norfloxacin antibiotics, respectively.

Quantitative biofilm formation

All twenty-four *Pseudomonas aeruginosa* isolates showed varying potential biofilm-forming capacities under identical experimental circumstances. Figure 5 illustrates the biofilm-producing capabilities of *P. aeruginosa*. Twenty-three isolates (95.8%) were strong biofilm producers, and one isolate (4.16%) was a moderate biofilm producer. These outcomes were attained following a 24-hour incubation period for the development and biofilm formation of *P. aeruginosa*. The results of the biofilm production in the presented study agree with the study of Lima and Morais [22]. *P. aeruginosa* is covered with extracellular polysaccharides (EPS) to provide a shield that protects the resident bacteria from external stress, phagocytosis, and provides them the ability to colonize and persist over time. Additionally, it offers a range of freely accessible products, such as nutrients, proteins, and enzymes for the biofilm community, and facilitates cellular communication [13].

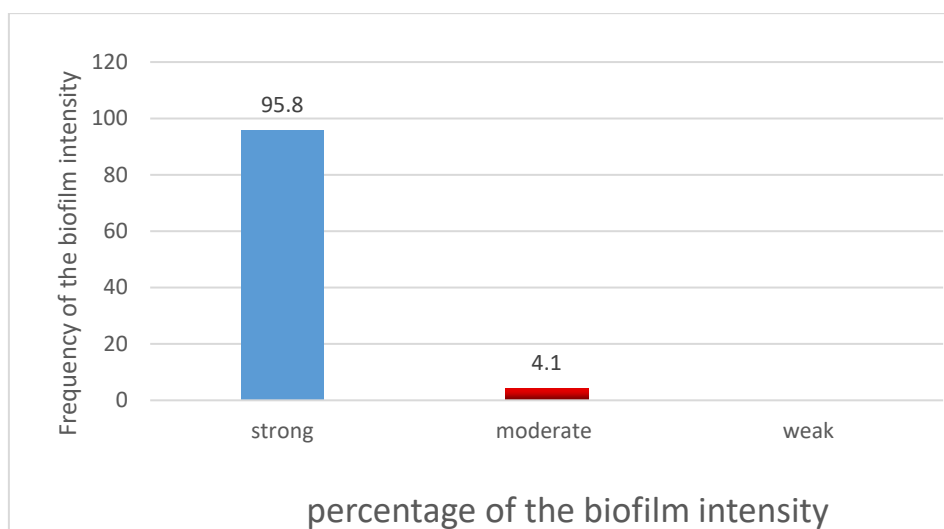


Figure 5: Percentage of *P. aeruginosa* biofilm intensity for microtiter plate assay.

Characterization of CuONPs

UV-visible spectral Analysis of CuONPs synthesized by the extracellular products of the Mixture of *K. pneumonia* and *S. aureus*.

The spectroscopic properties of the bio-synthesized CuO nanoparticles were analyzed utilizing UV-Vis spectroscopy. The synthesized CuONPs demonstrated significant UV absorption at approximately 682 nm. The aforementioned absorption may be mostly ascribed to the biosynthesis of copper oxide nanoparticles' direct band emissions, as shown in Figure 6. The results of the presented study agree with the study of Kumar [32]. The absorption of CuONPs at 682 nm is attributed to the electronic transition from the valence band region to the conduction band. Additionally, the optical properties of the nanoparticles are affected by a number of factors, including preparation methods, particle size, shape, and measurement methods[33].

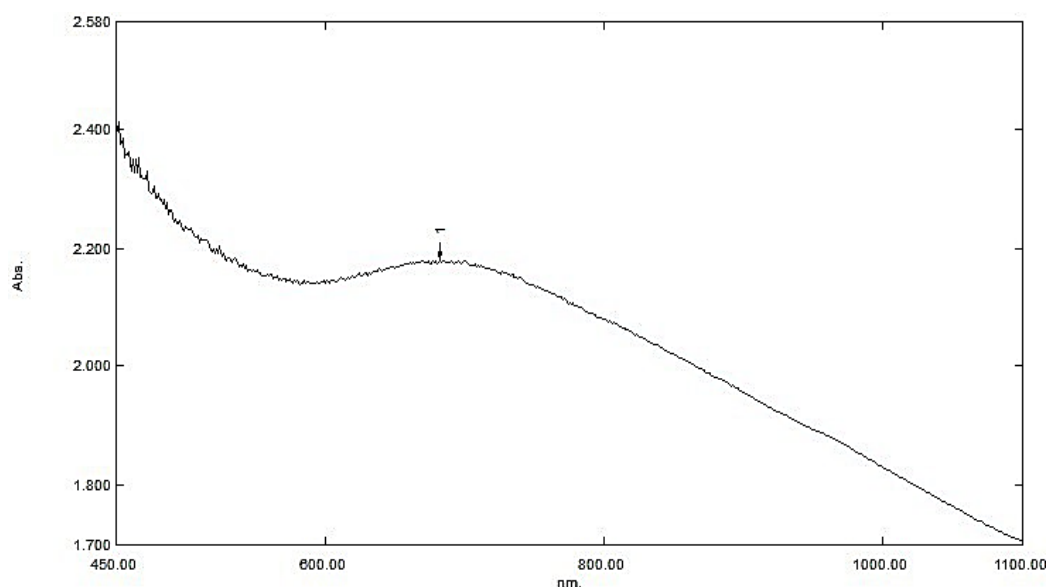


Figure 6: The UV-Visible absorption spectrum of CuO nanoparticles (CuO-NPs).

Fourier Transform Infrared (FTIR) analysis of CuONPs

The FTIR was performed to detect the functional group of the copper oxide nanoparticles. 3461.99-3224.76 cm^{-1} peaks range indicate the presence of H_2O , hydroxyl group H bonded OH

stretch. The peak at 1643.24 cm^{-1} may indicate the existence of alkenyl C=C stretch or may be NO_2 in the bacterial extract served in the reduction of Cu ions and copping of copper oxide [34]. $1556.45\text{--}1548.73\text{ cm}^{-1}$ peak may indicate the existence of aliphatic nitro compounds. $1442.66\text{--}1411.8\text{ cm}^{-1}$ peak is attributed to OH bending [35], or carbonate ion. 1049.20 cm^{-1} is attributed to the OH bending vibration [36]. The peaks 615.25 cm^{-1} and 482.17 cm^{-1} are attributed to the formation of the CuO vibration, which confirms the formation of the Copper oxide nanoparticles, as shown in Figure 7 [35]. Many studies exhibit that the peak at about 615 cm^{-1} is attributed to the stretch vibrations of CuO in the monoclinic crystalline structure, reflecting the crystalline formation of CuO. While the peak at about 482 cm^{-1} is indicated the CuO vibrations or crystalline lattice vibrations, a characteristic feature of copper oxide, these peaks are reported to be present in the fingerprint region. Therefore, these peaks in the FTIR spectrum can be considered evidence of CuONPs formation and a confirmation of the presence of Cu-O bonds in their crystalline structure[37].

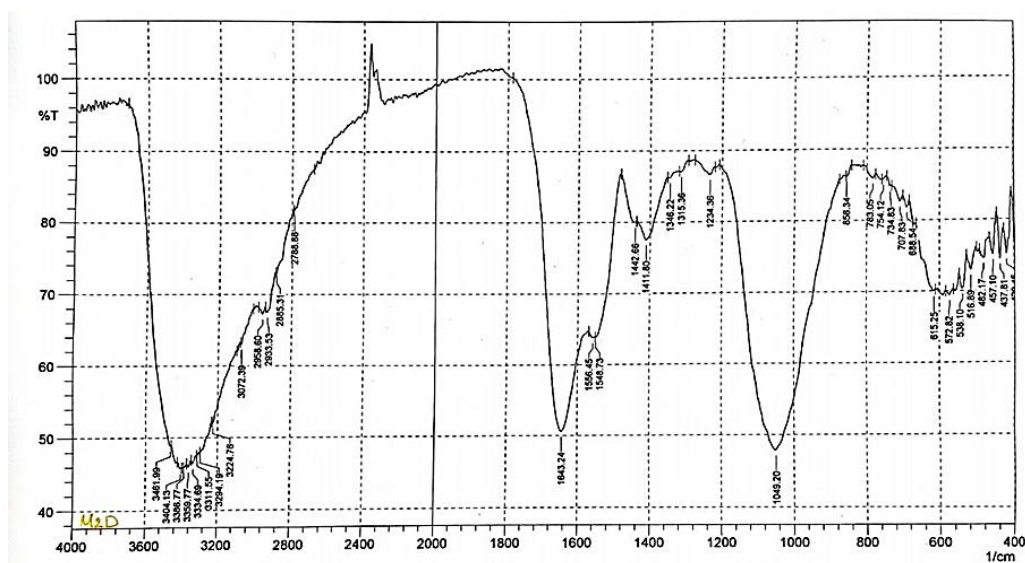


Figure 7: FTIR result of copper-oxide nanoparticles.

*Atomic force microscopy analysis of biosynthesized CuONPs using extracellular products of the mixture of *S. aureus* and *K. pneumonia*.*

The surface form generation of the CuONPs was examined using atomic force microscopy, showing that the 2D and 3D [18]. The images from AFM demonstrate that the bio-synthesized CuO NPs are spherical. AFM also recorded an average diameter of 62.64 nm . Figure 8 illustrates the two-dimensional and three-dimensional surface morphology of CuONPs. The result is in a correlation with Faris [38]. AFM result, which demonstrated that the average particle size of copper oxide nanoparticles was in the range from 30 nm to 90 nm .

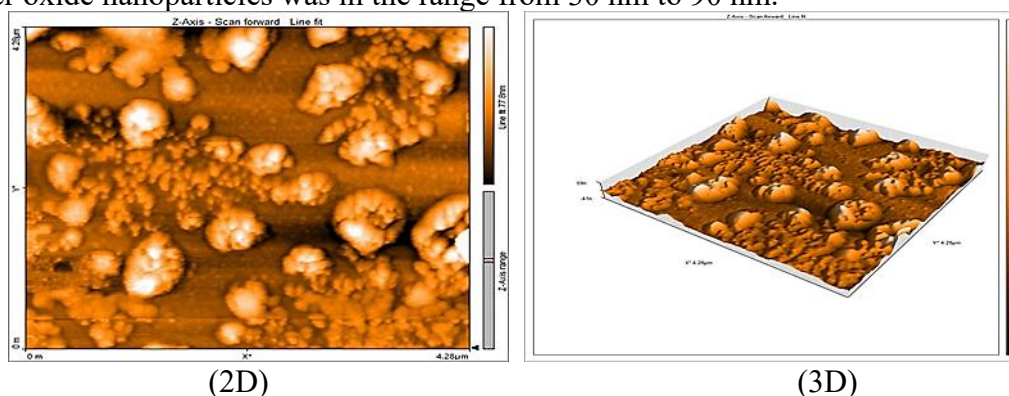


Figure 8: Atomic Force Microscopy (AFM) of bio-synthesized CuONPs

Field Emission-Scanning Electron Microscopy (FE-SEM)

The image of FE-SEM for the biosynthesized CuONPs exhibits uniform distribution and identical morphology consisting of spherical-shaped, composed of several interlinked sheet-ball-like crystalline structures, as shown in Figure 9. The average diameter = 52.48 was consistent with those of AFM. This result agreed with the FE-SEM result of Fakhredin *et al.*, [37], which reports that the CuONPs present in plate-like and big ball structures. These structures point to a well-organized growth or crystallization at the nanoscale. During the biosynthesis process, the bioactive compounds found in the bacterial supernatant, such as proteins, amino acids, and polyphenols, play a significant role as reducing and stabilizing agents. These compounds reduce copper ions (Cu^{2+}) to CuO and stabilize the resulting nanoparticles. The different concentrations of these compounds, as well as environmental conditions such as temperature and pH, affect the rate and direction of particle growth, leading to the formation of specific forms [38].

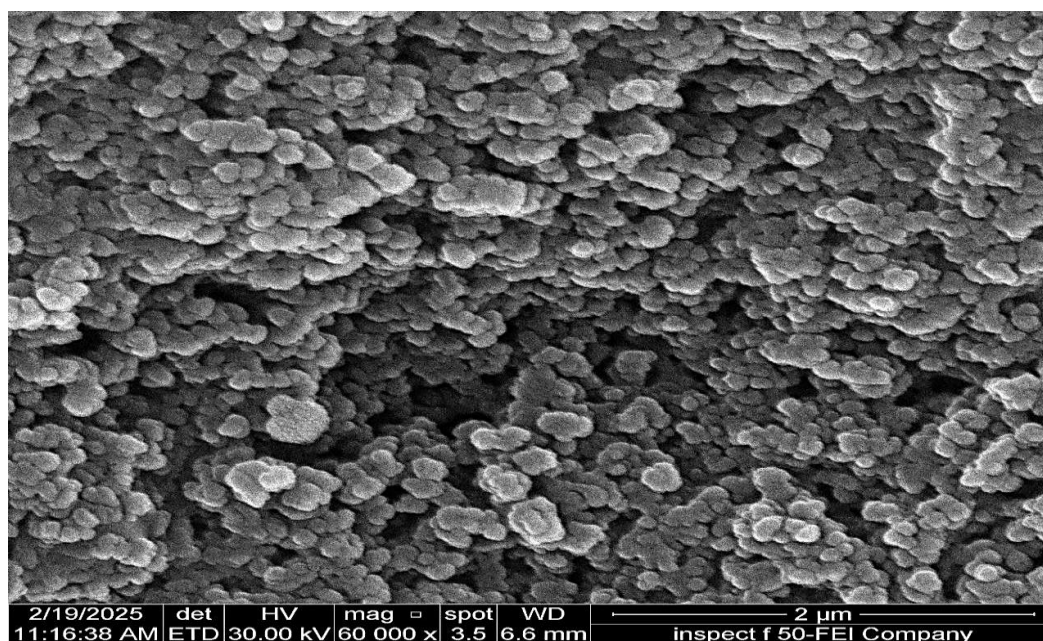


Figure 9: Field Emission Scanning Electron Microscopy image of biosynthesized CuONPs

X-ray Diffraction (XRD)

The results of the XRD of the biosynthesized CuO are shown in Figure 10. It signifies the presence of CuO with a monoclinic crystalline shape. The reflection pattern at 2θ is 32.16, 35.6, 38.53, 54.64, 58.29, 66.0, 68.7, and 75.0, illustrating the primary reflection of CuO that pertains to (110), (002), (111), (020), (202), (311), (113), and (004). The average crystalline size was 65.75 nm. The crystalline structure of the nanoparticles is responsible for the distinct and sharp peaks in XRD. Additionally, XRD confirmed the effective production of CuONPs and offered comprehensive details regarding their size and crystalline structure. The result of the presented study agreed with the XRD result of Rangasamy *et al.*, [39], which confirms the monoclinic crystalline shape of CuONPs.

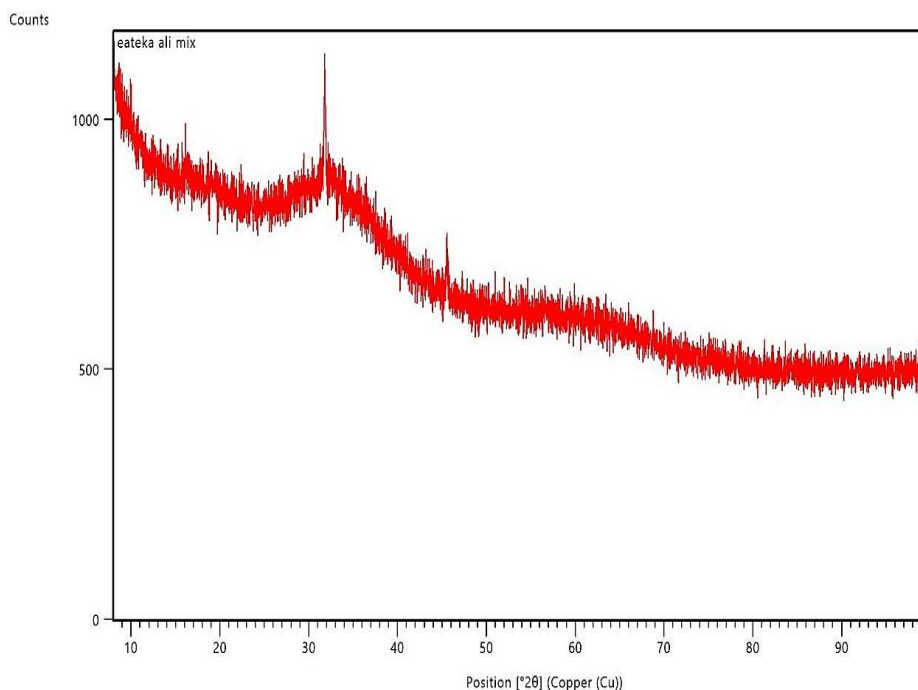


Figure 10: X- ray diffraction image of CuONPs.

The anti-biofilm activity of bio-synthesized CuONPs

The MIC test revealed that the last inhibitory concentration was 6.25 mg/ml. According to the study conducted by Abdelghafar, it was demonstrated that all doses exhibited antibacterial activity and could be assessed for antibiofilm efficacy [25]. The antibiofilm activity of CuONPs was assessed using a 96-well microtiter plate. CuONP was prepared in varying concentrations and employed as post-biofilm formation agent against the biofilm activity of *P. aeruginosa*. The findings indicate that the antibiofilm and antibacterial efficacy of CuONPs were directly correlated with concentration. The study's results demonstrated that all produced concentrations of CuO nanoparticles exhibit antibiofilm activity against *P. aeruginosa*. However, the highest activity was attained by the 50 mg/ml concentration (Figure 11). A study on CuO nanoparticles reported that CuONPs have efficacy against the initial adhesion and biofilm-forming bacteria cells, including *P. aeruginosa* [40].

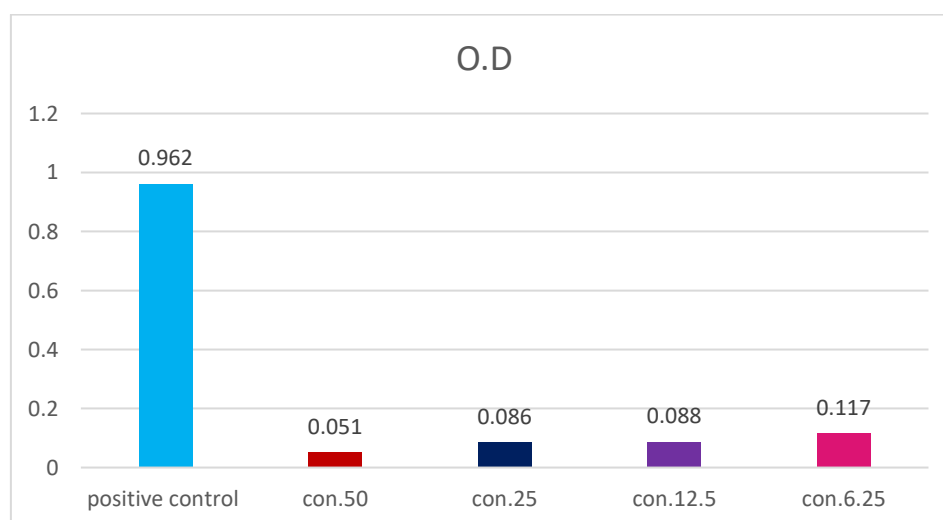


Figure 11: The results of the anti-biofilm efficacy of copper oxide nanoparticles.

Conclusion

The mixture of *K. pneumoniae* and *S. aureus* extracellular products was successfully used as reducing and stabilizing agents for biosynthesized CuONPs, which was confirmed using several techniques that exhibited an average diameter of 62.64 nm with a spherical structure, and the presence of CuO peaks. The biosynthesized CuONPs exhibit antibiofilm efficacy in all concentrations against the multidrug-resistant *P. aeruginosa*, with the highest anti-biofilm activity at 50 mg/ml.

Ethical approval

This study was ethically approved according to the reference number CSEC/1124/0109 by the ethical committee of the College of Science, University of Baghdad.

Conflict of interest

The authors declare that they have no conflicts of interest.

References

- [1] K. Deka, R. D. Nongbet, K. Das, P. Saikia, S. Kaur, A. Talukder, and B. Thakuria, "Understanding the mechanism underlying the green synthesis of metallic nanoparticles using plant extract(s) with special reference to Silver, Gold, Copper and Zinc oxide nanoparticles," *Hybrid Advances*, vol. 9, pp. 100399, 2025.
- [2] P. Pramanik, K. Dakua, T. Kar, R. Sahu, T. K. Dua, G. Nandi, S. Dey, A. Kumar, R. Khanra, and P. Paul, "Biosynthesis and in-vitro characterizations of copper oxide nanoparticle using *Mangifera indica* seed kernel extract and assessment of pharmacological properties," *Hybrid Advances*, vol. 8, pp. 100375, 2025.
- [3] A. Nagaveni, M. Anusuya, D. Santhanaraj, S. G. Gunasekaran, J. Gitanjali, S. Thangabalu, K. Krishnaveni, E. Jayanthi, and K. Rajakumar, "Tecoma stans intermediated green synthesis of copper oxide nanoparticles, their characterization, paracetamol degradation and biological activities," *Inorganic Chemistry Communications*, vol. 170, pp. 113503, 2024.
- [4] G. Velmathi, V. Sekar, N. S. Kavitha, M. F. Albeshr, and A. Santhanam, "Biosynthesis of gold nanoparticles by the extremophile bacterium *Deinococcus radiodurans* and an evaluation of its application in drug delivery," *Process Biochemistry*, vol. 145, pp. 250-260, 2024.
- [5] A. S. Dousari, M. Shakibaie, H. Hosseini-Nave, and H. Forootanfar, "Effect of biogenic bismuth nanoparticle on the expression of New Delhi metallo- β -lactamase (NDM) gene in Multidrug-Resistant *Klebsiella pneumoniae*," *Heliyon*, vol. 10, no. 12, 2024.
- [6] A. M. Collins, and R. Mizzi, "Virulence determinants in *Klebsiella pneumoniae* associated with septicaemia outbreaks in neonatal pigs," *Veterinary Microbiology*, vol. 302, pp. 110409, 2025.
- [7] A. A. Shah, A. S. S. Alwashmi, A. Abalkhail, and A. M. Alkahtani, "Emerging challenges in *Klebsiella pneumoniae*: Antimicrobial resistance and novel approach," *Microbial Pathogenesis*, vol. 202, pp. 107399, 2025.
- [8] N. H. Sayyid, and Z. R. Zghair, "Biosynthesis of silver nanoparticles produced by *Klebsiella pneumoniae*," *Materials Today: Proceedings*, vol. 42, pp. 2045-2049, 2021.
- [9] T. Wen, L. Meng, F. Zhao, Y. Shi, and T. Zhang, "Autocrine peptides inhibited the formation of VBNC state of *Staphylococcus aureus*," *Microbiological Research*, vol. 294, pp. 128103, 2025.
- [10] C. Malakar, B. Kashyap, S. Bhattacharjee, M. Chandra Kalita, A. K. Mukherjee, and S. Deka, "Antibiofilm and wound healing efficacy of rhamnolipid biosurfactant against pathogenic bacterium *Staphylococcus aureus*," *Microbial Pathogenesis*, vol. 195, pp. 106855, 2024.
- [11] S. Zhu, C. Hu, Y. Wang, M. Jin, Q. Zhang, S. Han, Y. Tang, D. Wu, D. Fu, S. Jiang, D. Song, L. Wei, W. Song, C. Zhang, and W. Zhang, "Daphnetin weakened the pathogenicity of methicillin-resistant *Staphylococcus aureus* by inhibiting Sortase A and α -hemolysin," *Biochimie*, vol. 229, pp. 84-94, 2025.
- [12] A. Ahmed Al-mehdhar, K. Mohammed Alarjani, N. Salem Aldosari, and M. Ahmed Alghamdi, "Antibacterial Efficacy of AgNPs synthesized from Aloe vera extract and *Staphylococcus*

- aureus Culture Supernatant,” *Journal of King Saud University - Science*, vol. 36, no. 10, pp. 103464, 2024.
- [13] M. T. T. Thi, D. Wibowo, and B. H. Rehm, “Pseudomonas aeruginosa biofilms,” *International journal of molecular sciences*, vol. 21, no. 22, pp. 8671, 2020.
- [14] N. F. H. Khorshid, and N. H. Odaa, “Optimum Conditions for Pyomelanin Production and Characterization from Local Isolates of Pseudomonas aeruginosa,” *Medical Journal of Babylon*, vol. 22, no. 1, pp. 108-116, 2025.
- [15] M. Naraki, P. Khodavandi, A. Khodavandi, and F. Alizadeh, “Efficacy of different microbial synthesized silver nanoparticles alone and in combination in single- and multi-species of Candida albicans and Pseudomonas aeruginosa biofilm inhibition and in downregulation of the HWP1 and PELA gene expression,” *Materials Today Communications*, vol. 42, pp. 111507, 2025.
- [16] K. I. A. Al-Masoudi, H. S. O. Al-Janabi, and H. T. M. Al-Mousawi, “Isolation and Characterization of Klebsiella pneumoniae from Urinary Tract Infections: A Comparative Study of Diagnostic Methods,” *SAR Journal of Pathology and Microbiology*, vol. 6, no. 1, pp. 1-7, 2025.
- [17] F. M. Ballah, M. S. Islam, M. L. Rana, F. B. Ferdous, R. Ahmed, P. K. Pramanik, J. Karmoker, S. Ievy, M. A. Sobur, and M. P. Siddique, “Phenotypic and genotypic detection of biofilm-forming Staphylococcus aureus from different food sources in Bangladesh,” *Biology*, vol. 11, no. 7, pp. 949, 2022.
- [18] M. Abd Qasim, and L. A. Yaaqoob, “Evaluation of antibacterial activity of iron oxide nanoparticles synthesis by extracellular lactobacillus against pseudomonas aeruginosa,” *Journal of medicinal and chemical sciences*, vol. 6, pp. 1100-1111, 2023.
- [19] H. M. Balasim, F. K. Emran, and L. A. Yaaqoob, “Biosynthesis of Iron Oxide Nanoparticles and Combination with Glyphosate Herbicide and Effect Against Cogon Grass Control,” *Diyala Agricultural Sciences Journal*, vol. 16, no. 1, pp. 145-158, 2024.
- [20] M. N. Abed, and H. M. Rasheed, “Effect of some sugars on carbapenemase gene expression in Pseudomonas aeruginosa,” *Plant Archives*, vol. 20, no. 1, pp. 181-186, 2020.
- [21] A. Mohamed, and F. Abdelhamid, “Antibiotic susceptibility of Pseudomonas aeruginosa isolated from different clinical sources,” *Zagazig Journal of Pharmaceutical Sciences*, vol. 28, no. 2, pp. 10-17, 2020.
- [22] J. L. d. C. Lima, L. R. Alves, J. N. P. d. Paz, M. A. Rabelo, M. A. V. Maciel, and M. M. C. d. Morais, “Analysis of biofilm production by clinical isolates of Pseudomonas aeruginosa from patients with ventilator-associated pneumonia,” *Revista Brasileira de terapia intensiva*, vol. 29, pp. 310-316, 2017.
- [23] N. A. A. S. T. Ahmed, and A. M. Almohaidi, “Investigation of biofilm formation ability and Assessment of cupB and rhlR Gene Expression in Clinical Isolates of Pseudomonas aeruginosa,” *Iraqi journal of biotechnology*, vol. 21, no. 2, pp. 641-650, 2022.
- [24] A. Wasilewska, U. Klekotka, M. Zambrzycka, G. Zambrowski, I. Świąćicka, and B. Kalska-Szostko, “Physico-chemical properties and antimicrobial activity of silver nanoparticles fabricated by green synthesis,” *Food chemistry*, vol. 400, pp. 133960, 2023.
- [25] A. Abdelghafar, N. Yousef, and M. Askoura, “Zinc oxide nanoparticles reduce biofilm formation, synergize antibiotics action and attenuate Staphylococcus aureus virulence in host; an important message to clinicians,” *BMC microbiology*, vol. 22, no. 1, pp. 244, 2022.
- [26] Z. Z. Khalaf, and I. J. Abed, “Evaluation the Antibacterial Effect of Rosemary and Lemon Grass Essential Oils against Planktonic and Biofilm of MRSA,” *Journal of Global Pharma Technology*, vol. 12, no. 06, 2009.
- [27] A. Y. Hussein, B. O. Abdulsattar, N. A. Al-Saryi, and W. H. Edrees, “Detection of some β -lactamase Genes in Klebsiella pneumoniae Isolated from some Baghdad Hospitals, Iraq,” *Al-Mustansiriyah Journal of Science*, vol. 35, no. 2, pp. 52, 2024.
- [28] O. H. Sheet, R. A. Talat, I. I. Kanaan, A. A. Najem, and A. S. Saeed Alchalabi, “Detection of the nuc gene in Staphylococcus aureus isolated from swamps and ponds in Mosul city by using PCR techniques,” *Iraqi Journal of Veterinary Sciences*, vol. 36, no. 3, pp. 821-824, 2022.

- [29] H. S. Auhim, and N. H. Odaa, "Molecular detection and the frequency of a pore-forming toxin in *Enterococcus faecalis* isolated from urinary tract infections," *Microbes and Infectious Diseases*, vol. 6, no. 2, pp. 948-956, 2024.
- [30] D. K. Govindarajan, and K. Kandaswamy, "Virulence factors of uropathogens and their role in host pathogen interactions," *The Cell Surface*, vol. 8, pp. 100075, 2022.
- [31] Z. Pang, R. Raudonis, B. R. Glick, T.-J. Lin, and Z. Cheng, "Antibiotic resistance in *Pseudomonas aeruginosa*: mechanisms and alternative therapeutic strategies," *Biotechnology advances*, vol. 37, no. 1, pp. 177-192, 2019.
- [32] Y. Kumar, V. Singh, A. Pandey, M. Genwa, and P. Meena, "Synthesis, characterization and antibacterial activity of ZnO nanoparticles."
- [33] M. I. Said, and A. Othman, "Structural, optical and photocatalytic properties of mesoporous CuO nanoparticles with tunable size and different morphologies," *Royal Society of Chemistry Advances*, vol. 11, no. 60, pp. 37801-37813, 2021.
- [34] M. Priya, R. Venkatesan, S. Deepa, S. S. Sana, S. Arumugam, A. M. Karami, A. A. Vetcher, and S.-C. Kim, "Green synthesis, characterization, antibacterial, and antifungal activity of copper oxide nanoparticles derived from *Morinda citrifolia* leaf extract," *Scientific Reports*, vol. 13, no. 1, pp. 18838, 2023.
- [35] A. M. Muslim, and I. S. Najji, "Green synthesis of CuO nanoparticles mediated *Rhazya stricta* plant leaves extract characterization and evaluation of their antibacterial and anticancer activity (in vitro study)," *Iraqi Journal of Physics*, vol. 22, no. 3, pp. 93-105, 2024.
- [36] R. Lu, W. Hao, L. Kong, K. Zhao, H. Bai, and Z. Liu, "A simple method for the synthesis of copper nanoparticles from metastable intermediates," *Royal Society of Chemistry Advances*, vol. 13, no. 21, pp. 14361-14369, 2023.
- [37] L. Gontrani, E. M. Bauer, A. Talone, M. Missori, P. Imperatori, P. Tagliatesta, and M. Carbone, "CuO nanoparticles and microaggregates: an experimental and computational study of structure and electronic properties," *Materials*, vol. 16, no. 13, pp. 4800, 2023.
- [38] R. A. Faris, "Synthesis, characterization, and optical properties of copper oxide thin films obtained by spray pyrolysis deposition," *Iraqi Journal of Physics*, vol. 11, no. 22, pp. 64-71, 2013.
- [39] M. Rangasamy, S. Gopal, A. Indhumathi, S. Loganathan, S. Manikandan, and R. Naresh, "Green synthesis and characterization of copper oxide nanoparticles using *Tecoma stans*," *Journal of Pharmaceutical Research international*, vol. 35, no. 7, pp. 9-16, 2023.
- [40] T. Khairy, D. H. Amin, H. M. Salama, I. M. A. Elkholy, M. Elnakib, H. M. Gebreel, and H. A. E. Sayed, "Antibacterial activity of green synthesized copper oxide nanoparticles against multidrug-resistant bacteria," *Scientific Reports*, vol. 14, no. 1, pp. 25020, 2024.